Journal of Organometallic Chemistry 693 (2008) 2397–2406

Contents lists available at ScienceDirect

Journal of Organometallic Chemistry

journal homepage: www.elsevier.com/locate/jorganchem

Synthesis and reactivity of rhodium(III) pentamethylcyclopentadienyl complexes of *N*–*B*–PTA(BH_3): X-ray crystal structures of [Cp^*RhCl_2{*N*–*B*–PTA(BH_3)}] and [Cp^*Rh{*N*–*B*–PTA(BH_3)}(η^2-CH_2 = CHPh)]

Sandra Bolaño [a,*], Alberto Albinati [b,*], Jorge Bravo [a], Maria Caporali [c], Luca Gonsalvi [c], Louise Male [b], M.[a] Mar Rodríguez-Rocha [a], Andrea Rossin [c], Maurizio Peruzzini [c,*]

[a] Departamento de Quimica Inorganica, Facultade de Quimica, Universidade de Vigo, Campus Universitario, E-36310 Vigo, Spain
[b] Department of Structural Chemistry (DCSSI) and School of Pharmacy, University of Milan, 21, via G. Venezian I – 20133 Milan, Italy
[c] Istituto di Chimica del Composti Organometallici, Consiglio Nazionale delle Ricerche (ICCOM–CNR), Via Madonna del Piano 10, 50019 Sesto Fiorentino, Florence, Italy

ARTICLE INFO

Article history:
Received 3 March 2008
Received in revised form 2 April 2008
Accepted 2 April 2008
Available online 10 April 2008

Keywords:
Water-soluble complexes
Rhodium
Hydrides
Boranyl phosphines
X-ray crystallography

ABSTRACT

The reaction between 1-boranyl-1,3,5-triaza-7-phosphaadamantane ligand *N*–*B*–PTA(BH_3) and [$Cp^*RhCl(\mu$-Cl)]$_2$ affords [Cp^*Rh{*N*–*B*–PTA(BH_3)}Cl_2] (**3**) or [Cp^*Rh{*N*–*B*–PTA(BH_3)}$_2$Cl]Cl (**5**) containing one or two P-bonded boronated PTA ligands. The hydride [Cp^*Rh{*N*–*B*–PTA(BH_3)}H_2] (**8**) was also obtained by reaction of **3** with $NaBH_4$ and alternatively by direct hydroboration of [$Cp^*Rh(PTA)Cl_2$] with excess $NaBH_4$. Moderately slow hydrolysis of the N-boranyl rhodium complexes affords dihydrogen, H_3BO_3 and the corresponding PTA derivatives, including the water-soluble dihydride [$Cp^*Rh(PTA)H_2$] (**9**). Finally, the reaction of **8** with electron poor alkynes gives the alkene complexes [Cp^*Rh{*N*–*B*–PTA(BH_3)}(η^2-CH_2 = CHR)] (R = Ph, **10**; C(O)OEt, **11**) as a mixture of rotamers η^2-coordinated to rhodium without affecting the N–BH_3 moiety. The X-ray crystal structures of **3** and **10** were also obtained and are here discussed.

1. Introduction

Water-soluble phosphines are among the preferred ligands used to impart solubility in water to transition metal complexes [1] and a variety of monodentate and polydentate hydrosoluble phosphines have been used over the years to generate homogeneous catalysts for applications to processes in water or biphasic water/organic solvent conditions [2].

Among monodentate phosphines, a special role is played by the neutral cage-like ligand 1,3,5-triaza-7-phosphaadamantane (PTA) (**I**) originally synthesised by Daigle et al. in 1974 [3] and used in the following three decades to prepare an assortment of water-soluble transition metal complexes to be used as homogeneous aqueous phase catalysts and as luminescent materials when coordinated to gold precursors [4].

During the last few years a renewed interest for PTA and its chemistry has been stimulated by the increasing attention to chemical sustainable processes aimed at minimizing waste and environmental impact [5], and by the recent findings that transition metal PTA complexes, mainly ruthenium [6,7] but also osmium [8], rhodium [8] and platinum [9], are endowed with remarkable binding activity towards both DNA and proteins showing cytotoxicity towards selected tumour cells. More recently, research has focused on modifications of PTA motif as subtle changes of the electronic and steric requirements of the phosphaadamantane skeleton may help in the tailored synthesis of efficient catalysts for various applications.

The most straightforward modifications of PTA bottom rim have been generally achieved by reaction with electrophiles, including alkyl halides [10] (**II**) and anhydrides (**III**) [11]. Double quaternization of the PTA ligand has been recently demonstrated (**IV**) [12], while opening of the PTA cage has resulted in bidentate P,N- (**V**) [13] and N,N-ligands (**VI**) [12], which, in the former case, have been used by some of us to prepare rhodium catalysts active in biphasic alkene hydroformylation [14]. Neutral Lewis-acids may represent target reagents towards the functionalization of PTA and in recent reports our group [15], Frost et al. [16] have separately shown that borane binds PTA with up to four BH_3 groups, *i.e.* on both nitrogen and phosphorus atoms. In this contribution, we report findings on the coordination chemistry of mono- and bis-boranyl PTA towards Cp^*Rh synthons forming a variety of boronated-PTA rhodium complexes. These complexes can undergo different reactions resulting in the formation of boronated-PTA rhodium hydrides and π-alkene complexes, as demonstrated by NMR experiments and X-ray crystallographic studies.

* Corresponding authors. Tel.: +39 0555225289; fax: +39 0555225203.
E-mail addresses: mperuzzini@iccom.cnr.it, peruz@fi.cnr.it (M. Peruzzini).

0022-328X/$ - see front matter © 2008 Elsevier B.V. All rights reserved.
doi:10.1016/j.jorganchem.2008.04.006

2. Results and discussion

2.1. Synthesis and characterization of rhodium PTA boranyl complexes

The straightforward reaction of the 1-boranyl-1,3,5-triaza-7-phosphaadamantane ligand *N*–*B*–PTA(BH_3) [16] with [Cp^*RhCl-(μ-Cl)]$_2$ (**1**) in a 2:1 mol ratio in THF affords, after work-up, the new complex [Cp^*Rh{*N*–*B*–PTA(BH_3)}Cl_2] (**3**) which was isolated in excellent yield as an air stable orange microcrystalline solid with analytical data in agreement with the proposed formulation (Scheme 1). Alternatively, compound **3** can be prepared in comparable yield by treatment of the known [Cp^*Rh(PTA)Cl_2] complex (**2**) [8] in THF with a stoichiometric amount of BH_3.THF. Apart from microanalytical data, the presence of the aminoborane moiety in **3** was determined by IR and NMR spectroscopy. The IR spectrum of **3** shows stretching vibrations ascribable [17] to both ν_{BH} at 2372, 2316, 2273 cm^{-1} and ν_{BN} at 1176 cm^{-1}, while the ^{11}B NMR spectrum ($CDCl_3$) exhibits a broad resonance at −9.85 ppm only slightly deshielded with respect to the free *N*-boronated phosphine [δ = −10.55]. Noticeably, coordination to rhodium of the *N*-boranyl phosphine broadens the ^{11}B resonance ($\omega_{1/2}$ = 345 Hz) which does not show any discernable coupling to BH_3 protons. In keeping with P-coordination to rhodium of the phosphaadamantane [18], the $^{31}P\{^1H\}$ NMR spectrum exhibits a doublet at −29.2 ppm with $^1J_{PRh}$ = 147 Hz consistent with a Rh(III) metal centre [8]. The ^1H NMR spectrum displays a broad three protons resonance (0.9–1.5 ppm) corresponding to the BH_3 group bound to the N atom. The other proton resonances agree with the proposed formulation and do not deserve additional comment confirming the lack of C_3 symmetry for the 12 CH_2 protons of the PTA backbone (3.7–4.6 ppm) upon quaternization of one nitrogen atom (see Scheme 2).

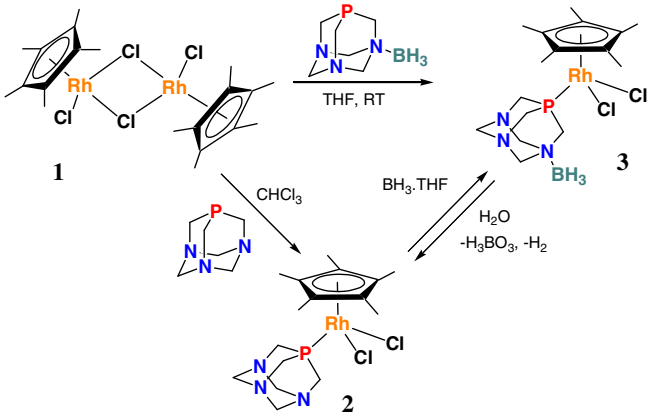

Scheme 1.

The solid-state structure of compound **3** proved difficult to refine satisfactorily due to the poor quality of the crystals (obtained by slow evaporation of a diluted acetone solution) and the disorder arising from the Cp^* ring (*cf.* Section 4). Nevertheless, there is no question as to the overall structure of complex, confirming the structural formulation as shown in Fig. 1. Selected bond lengths and angles are listed in Table 1.

The coordination around the rhodium atom can be described as a three-legged piano stool defined by the Cp^* ligand, the *N*-boronated PTA phosphine and two chloride atoms. The Rh–P bond length in **3** [2.268(4) Å] is significantly longer than that in [Rh(PTA){PTA(H)}$_3$Cl]Cl_2, with a Rh–P separation at 2.206(1) Å [19], but identical to that in [Cp^*Rh{$P(OEt)_3$}Cl_2] [20] [2.268(3) Å] and similar to that found in **2** [2.286(1) Å] [8].

Compound **3** is the third transition metal complex of the recently prepared 1-boranyl-PTA ligand [21] and its synthesis confirms that boranyl adducts of the popular phosphaadamantane PTA may be used to obtain another class of ligands to bind transition metal fragments. Alternatively, the reaction of **2** with borane, which also results in the formation of **3**, suggests that this class of ligands may be directly assembled via simple boronation of *P*-bonded PTA ligands. As for the free 1-boranyl-1,3,5-triaza-7-phosphaadamantane molecule [15], **3** is unstable in water and slowly reverts back to **2** releasing one equivalent of orthoboric acid when water is added to a MeOH or Me_2CO solution of **3** [22]. By contrast,

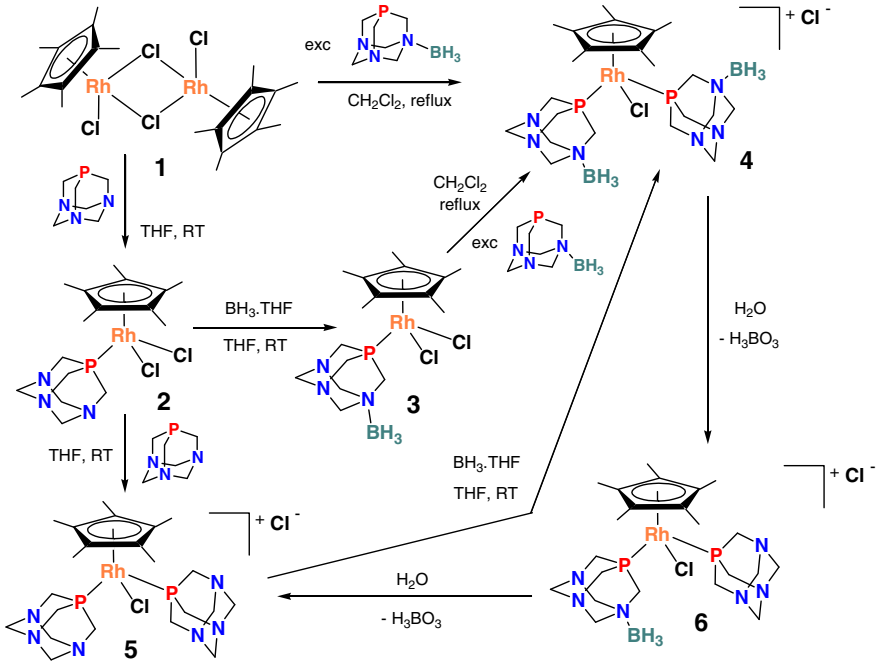

Scheme 2.

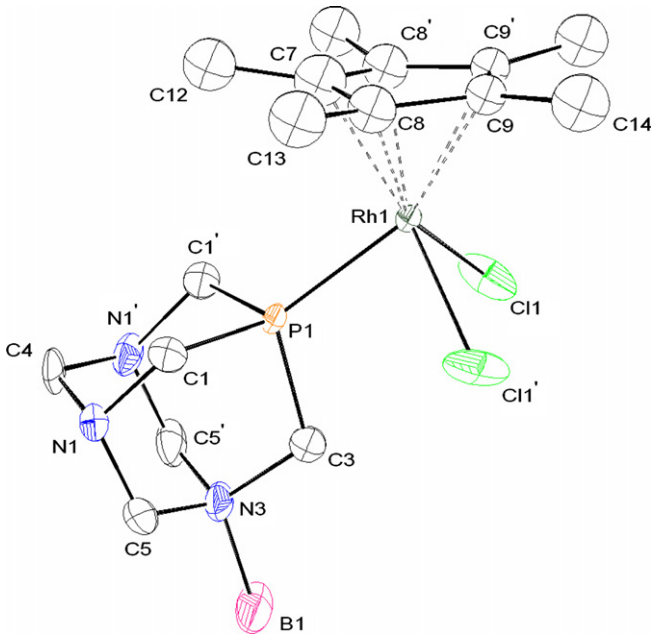

Fig. 1. ORTEP plot of complex **3** (Hydrogen atoms omitted for clarity; ellipsoids drawn at 50% probability).

Table 1
Selected bond lengths (Å) and angles (°) for **3**

Rh–cp*[a]	1.80 (3)	P1–Rh1–Cl1	87.3[a]
Rh1–C11	2.391 (3)	P1–Rh1–Cl1′	87.3[a]
Rh1–P1	2.268 (4)	Cl1–Rh1–Cl1′(2)	91.4[b]
Rh1–C7	2.13 (4)	P1–Rh1–cp*	129.8 (7)
Rh1–C8	2.07 (2)	Cl1–Rh1–cp*	124.5 (6)
Rh1–C9	2.21 (1)		
N3–B1	1.64 (2)		

[a] cp* refers to the centroid of the Cp* ligand.
[b] Primed atoms are obtained by those unprimed by the symmetry operation: *x*, 1/2 −*y*, *z*.

solutions of **3** in dry polar solvents (MeOH, Me_2CO, THF, CH_2Cl_2) are indefinitely stable when exposed to air.

The bis-boranyl-PTA derivative [Cp*Rh{*N*–*B*–PTA(BH_3)}$_2$Cl]Cl (**4**) was obtained by reacting **1** with *N*–*B*–PTA(BH_3) in a 1:4 molar ratio in refluxing dichloromethane. Monitoring of the reaction by $^{31}P\{^1H\}$ NMR spectroscopy shows the presence of pure **4** in solution without additional signals. However, work-up of the solution at room temperature gives a yellow powder whose analytical data do not perfectly match the proposed formula (see Section 4). On redissolving **4** in DMSO at room temperature, $^{31}P\{^1H\}$ NMR shows that the bis-boranyl adduct slowly reverts into **3** with loss of one *N*–*B*–PTA(BH_3) ligand, hence cannot be isolated in pure form but rather as a mixture of **4** and **3** in the approximate 9:1 ratio. In contrast, the bis-PTA complex [Cp*Rh(PTA)$_2$Cl]Cl (**5**) is indefinitely stable in solution [8]. At first glance, there is no simple rationale to account for the observed instability of **4** which can hardly be attributed exclusively to electronic factors associated with the *N*-boronation of PTA. We believe that steric reasons (crowding of the piano stool ligands) may be also important in determining the instability of **4**. Direct boronation of **5** in THF using a slight excess of $BH_3 \cdot$ THF or reaction of **3** with excess of boronated PTA also affords **4** in fairly good yield.

In line with the proposed formula, the $^{31}P\{^1H\}$ NMR spectrum of **4** displays a doublet at −32.5 ppm with a $^1J_{PRh}$ = 135 Hz. Consistently, the ^1H NMR spectrum shows, apart from a broad signal between 0.98 and 1.40 ppm for the six BH_3 protons and the expected uninformative multiplets (3.85–4.71 ppm) due to the PTA methylene protons, a triplet at δ 1.83 ($^4J_{HP}$ = 3.3 Hz) assigned to the methyl Cp* protons coupled to the two P atoms.

When dissolved in wet DMSO-d_6, complex **4** slowly hydrolyses to give a mixture of **5** and the mixed PTA–PTA(BH_3) species [Cp*Rh{*N*–*B*–PTA(BH_3)}(PTA)Cl]$^+$ (**6**) [$^{31}P\{^1H\}$ NMR: δ_{PTA} = − 34.1, $\delta_{\{N-B-PTA(BH_3)\}}$ = 34.2; $^2J_{PP}$ = 135.7 Hz]. On standing, complex **6** slowly converts to **5** with release of H_3BO_3. No attempt was made to isolate pure **6** in the solid state.

We have previously observed that multiple boronation of PTA is possible and, depending on the PTA/BH_3 ratio, up to 4 equiv. of borane may be coordinated to the four heteroatoms of the triazaphosphaadamantane molecule [15]. Attempts to incorporate more than one BH_3 unit on the same PTA molecule once coordinated to a transition metal were however only partially successful (Scheme 3). When a THF solution of **2** was reacted at room temperature with 2.5 equiv. of $BH_3 \cdot$ THF and the progress of the reaction monitored by $^{31}P\{^1H\}$ NMR spectroscopy, a new signal at −30.9 ppm (d, $^1J_{PRh}$ = 152 Hz) was observed. This product was isolated as an orange solid that slowly decomposes even if kept under inert atmosphere. Although the low stability of this compound in the solid state did not allow to obtain good analytical data, its spectroscopic features agree with the occurrence of a double *N*,*N*′-boronation of

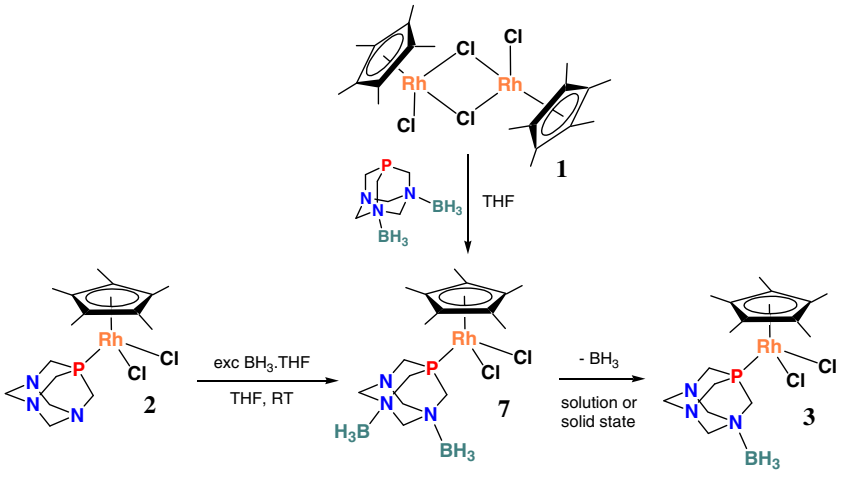

Scheme 3.

the rhodium-coordinated PTA [23]; thus, we assign the formula [Cp^*Rh{*N*–*B*–PTA(BH_3)$_2$}Cl_2] (**7**). Once redissolved in DMSO-d_6, the ^{1}H NMR spectrum of **7** displays a broad resonance (0.89–1.44 ppm) for the six BH_3 hydrogens, a doublet at 1.67 ppm (Cp^*_{Me}) and several multiplets at (3.7–4.6 ppm) ascribable to the PTA protons. All these signals coexist in solution with those of compound **3**, indicating that compound **7** easily undergoes partial deboronation yielding the monoboronated species **3** unless an excess of borane is maintained in the solution. The deboronation process is faster in DMSO solution than in the solid state and is completed in about 2 h giving **3** as the only detectable species. Addition of degassed water to a DMSO solution of **7** greatly accelerates the process which eventually affords the deboronated PTA complex **2**.

In keeping with our analysis, the reaction of the dimer **1** in $CDCl_3$ with excess *N*–*B*–PTA(BH_3)$_2$, in NMR tube scale gave **7**, indicating that also the bis-boronated phosphine may behave as a ligand.

2.2. Synthesis and characterization of the rhodium hydrides [Cp^*Rh{ *N*–*B*–PTA(BH_3)}H_2] (**8**) and [Cp^*Rh(PTA)H_2] (**9**)

Hydrosoluble rhodium hydride complexes are an underrepresented class of organometallic complexes [24], thus we decided to investigate the reaction of **2** with $NaBH_4$ which is one of the most common reagents to convert rhodium halides into the corresponding hydrides [25]. However, treatment of **2** in EtOH with a large excess of $NaBH_4$ did not give the expected dihydride complex [Cp^*Rh(PTA)H_2] (**9**). Instead, the dihydride [Cp^*Rh{*N*–*B*–PTA(BH_3)}H_2] (**8**) was obtained, where a BH_3 ligand has been selectively delivered to one of the PTA nitrogen atom (Scheme 4). Compound **8** can also be obtained by reacting the *N*-boranyl complex **3** with $NaBH_4$ under the same reaction conditions. The hydride **8** is a brownish red solid, stable only if kept under inert atmosphere.

The IR spectrum of **8** shows characteristic ν_{BH} bands at 2371, 2318, 2275 cm^{-1}, a ν_{BN} band at 1170 cm^{-1} and a medium intensity ν_{RhH} band at 1964 cm^{-1}. The ^{31}P{^{1}H} NMR spectrum displays a doublet at −18.5 ppm ($^1J_{PRh}$ = 155 Hz) which transforms into a doublet of triplets ($J_{PH(residual)}$ = 43 Hz) when an off-resonance experiment is performed, confirming the presence of two magnetically equivalent hydride ligands coordinated to the rhodium atom. The ^{1}H NMR spectrum displays, apart from the signals corresponding to the Cp^* and *N*–*B*–PTA(BH_3) ligands, a high field doublet of multiplets (δ = −13.67; $^2J_{PH}$ = 43 Hz, $^1J_{RhH}$ = 27 Hz, $^4J_{HH(Me)}$ = 1.1 Hz) integrating by two protons and assignable to the two hydride ligands (Fig. 2, right). These exhibit a $T_{1(min)}$ value of 532 ms at 400 MHz (acetone-d_6, 193 K) confirming their classical nature [26]. The multiplets due to the boronated PTA ligand range from 4.20 to 3.40 ppm and suggest a loss of the ternary PTA symmetry due to the boronation of one of the nitrogen atoms. This lack of symmetry is reflected also in the ^{13}C{^{1}H} NMR spectrum which displays two pairs of CH_2 resonances. Computer simulation [27] of the spectrum and a perusal of 2 D ^{1}H,^{13}C-HMQC, ^{1}H,^{1}H-COSY and ^{1}H,^{1}H-NOESY spectra allowed us to fully assign the proton and carbon resonances (see sketch **VII** below for the labelling scheme used and Section 4 for details) and disclose the otherwise practically invisible BH_3 resonance. Indeed, these three protons give rise to a very broad signal centred at 2.07 ppm extended over 400 Hz, which correlates only to the H_α and the two diastereotopic $H_{\gamma'}$ and $H_{\gamma''}$ protons in the ^{1}H,^{1}H-NOESY spectrum (Fig. 3).

The presence of N-bonded BH_3 was eventually confirmed by the ^{11}B NMR spectrum displaying a broad quartet at δ = −10.8 ($^1J_{HB}$ = 85 Hz).

The *N*-boranyl PTA hydride is unstable in chlorinated solvents where it quickly reverts to **3**, whereas solutions of **8** in benzene, toluene and acetone are stable for several days when stored under an inert atmosphere.

Full deboronation of **8** takes place by adding an excess (0.4 mL, 300 equiv.) of degassed water to an acetone-d_6 solution in a NMR tube and heating to *ca.* 60 °C for 20 h. Hydrolytic removal of BH_3 from **8** affords a slightly high field shifted doublet in the ^{31}P{^{1}H} NMR spectrum (δ = −20.2 ppm, doublet, $^1J_{PRh}$ = 147 Hz) which is consistent with the formation of the rhodium dihydride [Cp^*Rh(PTA)H_2] (**9**) in quantitative NMR yield. Formation of H_3BO_3 (^{11}B NMR: δ = 19.5, s) [15,22] and evolution of dihydrogen (^{1}H NMR: δ = 4.64, s) accompany the cleavage of the N_{PTA}–BH_3bond of **8** similarly to what shown by both **5** and the free ligand. Accordingly, a new set of hydride resonances (dd) appears in the high field region of the ^{1}H NMR spectrum (δ = −14.44 ppm; $^2J_{HP}$ = 42 Hz and $^1J_{HRh}$ = 28 Hz) replacing the multiplet of **8** (Scheme 4).

Independent synthesis of **9** (NMR tube scale) by treatment of a solution of **2** in benzene-d_6 with one equivalent of sodium bis(2-methoxyethoxy)aluminium hydride, *i.e.* Red-Al, a hydrurating reagent comparable with $LiAlH_4$ that does not contain boron atoms (Scheme. 5), confirmed the NMR data set observed in the previous experiment generating **9** by selective N–B hydrolysis of **8** [28].

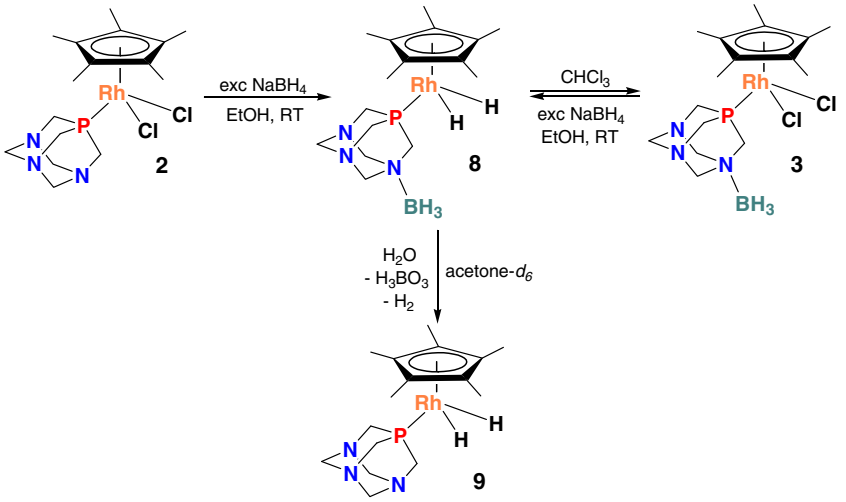

Scheme 4.

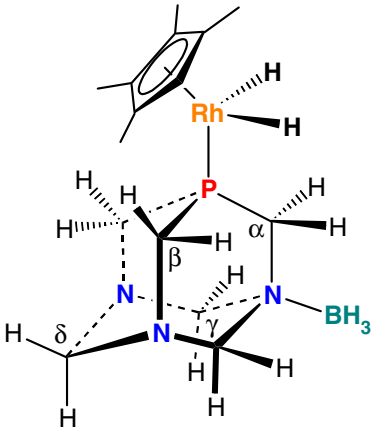

VII

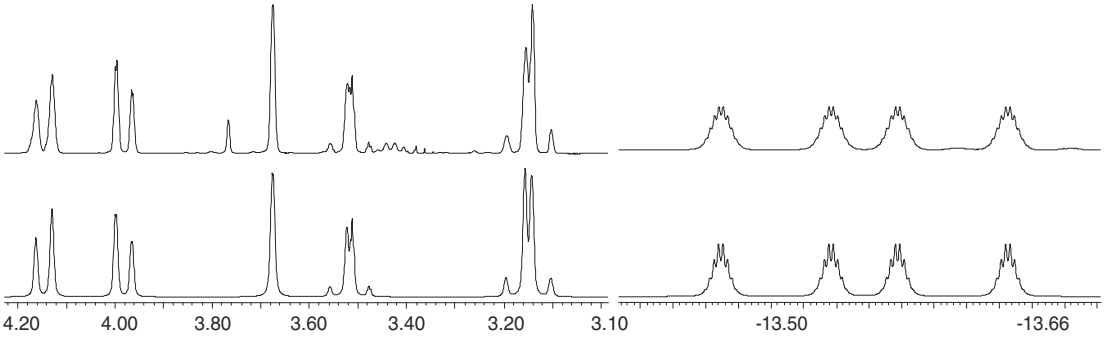

Fig. 2. Experimental (top) and simulated (bottom) ^{1}H NMR spectrum of compound **8** (C_6D_6, 294 K, 400.13 MHz).

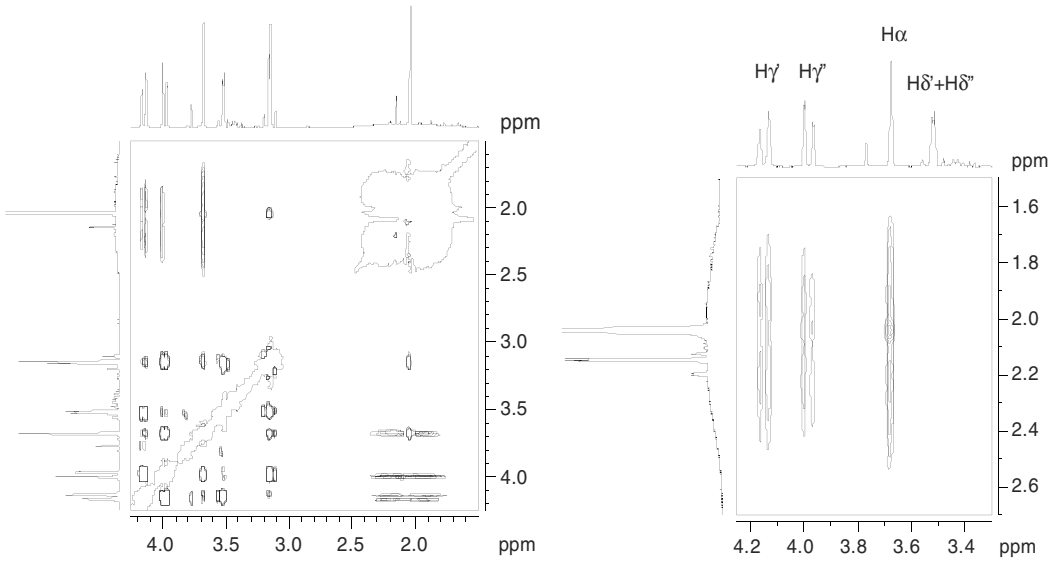

Fig. 3. ^{1}H NOESY spectrum of **8** (C_6D_6, 294 K, 400.13 MHz). Broad NOE signals allow to assign the resonances of BH_3 protons and to confirm the presence of this fragment in the molecule.

*2.3. Reactivity of **8** with alkynes: synthesis of Rh(I) complexes [Cp*Rh{N–B–PTA(BH$_3$)}(η^2-CH$_2$ = CHPh)] (**10**) and [Cp*Rh{N–B–PTA(BH$_3$)}{η^2-CH$_2$ = CHC(O)OEt}] (**11**)*

In order to verify whether the PTA-boranyl coordinated molecule may undergo further reactivity at the ancillary ligands, we investigated the reactions of the dihydride **8** towards typical organic substrates capable of reacting with rhodium hydrides. Electron poor alkynes are suitable reagents for electrophilic activation of Rh–H bonds. Generally, the reaction results in the formation of insertion products with different regio- and stereochemistry strongly depending on the electronic nature of the alkyne and reaction conditions [29].

The dihydride [Cp*Rh{*N*–*B*–PTA(BH$_3$)}H$_2$] (**8**) reacts with a slight excess of activated alkynes, such as phenylacetylene or ethyl propiolate HC≡CC(O)OC$_2$H$_5$ in C_6H_6 to give the π-alkene complexes

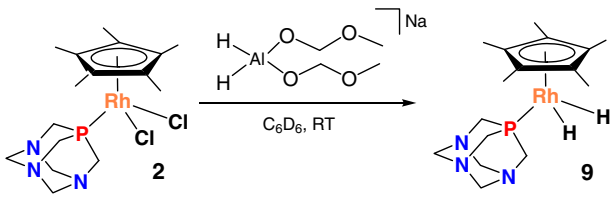

Scheme 5.

[Cp*Rh{*N*–*B*–PTA(BH$_3$)}(η^2-CH$_2$ = CHPh)] (**10**) and [Cp*Rh{*N*–*B*–PTA(BH$_3$)}{η^2-CH$_2$ = CHC(O)OEt}] (**11**), respectively (Scheme 6). Complexes **10** and **11** are orange solids stable at room temperature if stored under an inert atmosphere. As expected from the different electronic properties of the two alkynes, the reaction takes place immediately with ethylpropiolate whereas the less activated HC≡CPh reacts only after heating the solution to about 60 °C. Although no intermediate product was observed by *in situ* NMR monitoring of the process, it is likely that the reaction proceeds via alkyne insertion across one Rh–H bond to give a Rh(hydrido)vinyl species. Such species have been detected in a few cases [30], including for the related rhodium complexes [Cp*Rh(PMe$_3$)(HRC = CHR)] for which a detailed mechanistic study was undertaken [29].

Both ^{31}P{^{1}H} NMR spectra of compounds **10** and **11** feature two doublets in the ratio 1:4 (**10**) (δ = – 31.6 ppm, $^1J_{PRh}$ = 206 Hz; δ = – 36.9 ppm, $^1J_{PRh}$ = 214 Hz) and 1:9 (**11**) (δ = –32.4 ppm, $^1J_{PRh}$ = 198 Hz; δ = –35.2 ppm, $^1J_{PRh}$ = 207 Hz) indicating the presence of two different Rh(I) species tentatively assigned as rotamers of the η^2-alkene complexes [29a,31]. Increasing the temperature to 80 °C in toluene-d_8, the ^{31}P NMR spectra did not show coalescence of the rotamers resonances neither for **10** nor for **11**, thus suggesting a high-energy rotational barrier.

The ^{1}H NMR spectra of both compounds show the disappearance of the high field hydride signals and confirm the formation of two structurally related blocked rotamers of the η^2-alkene complexes. Although a close superimposition of the NMR resonances of the rotamers in both ^{1}H and ^{13}C NMR spectra does not allow a complete assignment of the NMR spectrum of the less abundant rotamers, a series of heterocorrelated ^{13}C-^{1}H 2D-NMR experiments has permitted to assign the ^{1}H and ^{13}C{^{1}H} NMR signals for the major rotamers of the two compounds.

The reaction of **8** with terminal alkynes does not affect the N-boranyl functionality of the coordinated boronated-PTA as confirmed by both IR spectroscopy, showing the typical absorptions of the N–BH$_3$ moiety, and ^{11}B{^{1}H} NMR spectroscopy, displaying a broad signal at δ = –10.9 (**10**) and δ = –10.4 (**11**). Remarkably, no differentiation of the two rotamers was evident from the boron NMR spectra, likely reflecting the negligible difference of the two *N*–*B*–PTA(BH$_3$) borane atoms in the two rotamers.

Crystals of **10** were obtained from slow evaporation of a diluted benzene solution. An ORTEP view of this complex is shown in Fig. 4 together with the labelling scheme while selected bond distances and angles listed in Table 2. The coordination sphere consists of the a Cp* ligand, the P-coordinated *N*–*B*–PTA(BH$_3$) phosphine and the π-coordinated styrene ligand.

The distances Rh–C(Cp*) are not equivalent, with two separations Rh1–C9 and Rh1–C11 (at 2.293(9) Å and 2.19(1) Å, respectively) being significantly different from the others, likely caused by the PTA-boranyl ligand. For the BH$_3$ coordinated to one of the three nitrogen atoms of PTA, the N–B separation at 1.61(1) Å is comparable to that found both in the coordinated and uncoordinated boronated cage [1.58(2) Å] [16]. All other distances fall in the expected range [32].

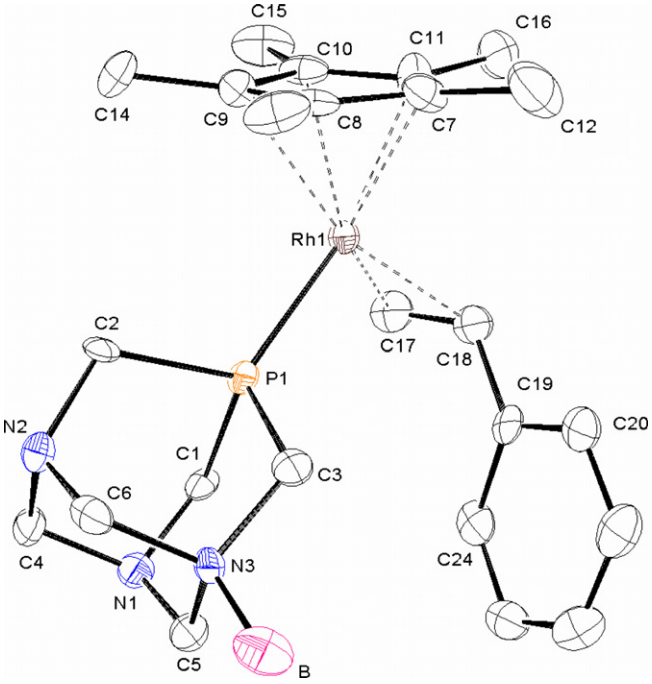

Fig. 4. ORTEP view of complex **10** (Hydrogen atoms omitted for clarity; ellipsoids drawn at 50% probability).

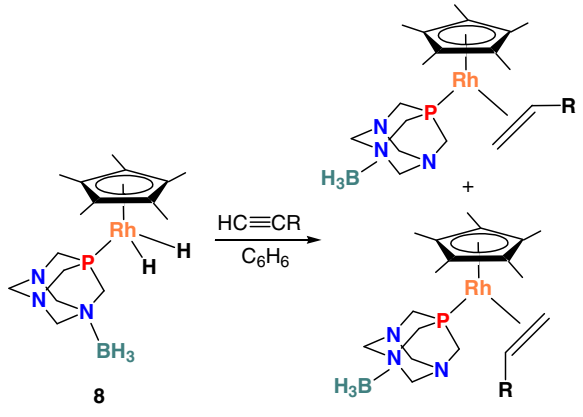

R= Ph, 10; C(O)OEt, 11

Scheme 6.

Table 2
Bond lengths (Å) and angles (°) for **10**

Rh1–P1	2.217 (2)	Rh1— P1–C1	125.2 (3)
Rh1–C7	2.269 (9)	Rh1–P1–C2	117.7 (3)
Rh1–C8	2.265 (9)	Rh1–P1–C3	117.6 (3)
Rh1–C9	2.293 (9)	P1–Rh1–cp*	131.4 (4)
Rh1–C10	2.265 (9)	cp*–Rh1–C17	131.3 (7)
Rh1–C11	2.19(1)	cp*–Rh1–C18	128.2 (8)
Rh1–C17	2.098 (9)	C17–C18–C19	127.3 (9)
Rh1–C18	2.143 (9)	B1–N3–C3	110.7 (7)
Rh1–cp*[a]	1.90 (1)	B1–N3–C5	110.1 (7)
P1–C$_{av}$[b]	1.836 (9)	B1–N3–C6	110.0 (7)
B1–N3	1.61 (1)		
C17–C18	1.40 (1)		
C18–C19	1.47 (1)		

[a] Cp* refers to the centroid of the Cp* ligand.
[b] P1–C$_{av}$ refers to the average P–C bond length involving the P-atom and the three methylene carbons of the PTA cage, namely C1, C2 and C3.

3. Conclusions

In this paper, we have described the synthesis and characterization of a new family of rhodium complexes containing the *N*–boranyl PTA(BH_3) cage-like phosphine as a monodentate P-coordinated ligand. The PTA-boronated complexes may be prepared either by direct reaction of the N-boranyl PTA adduct with suitable rhodium(III) precursors or by *in situ* boronation of the PTA derivatives. Remarkably, the *N*–boranyl PTA complexes tolerate a variety of chemical transformations including the reaction with hydride sources such as $NaBH_4$ terminally yielding a rhodium dihydride. As determined for the free ligand, the N–BH_3 moiety does not survive hydrolytic conditions, but the hydrolysis is much slower than that observed for the free boronated molecule.

4. Experimental

4.1. General procedures

All synthetic procedures were carried out using standard Schlenk glassware under an inert atmosphere of dry argon. The ligands PTA [3] and *N*–*B*–PTA(BH_3) [15] and the complexes [$Cp^*RhCl(\mu\text{-}Cl)]_2$ [33], and [$Cp^*Rh(PTA)Cl_2$] [8] were prepared as described in the literature. Other reagents were obtained from commercial suppliers and used without further purification. Solvents were distilled and degassed according to standard procedures [34]. Infrared spectra (KBr discs) were recorded on a Bruker Vector IFS 28 FT apparatus. ^1H, $^{31}P\{^1H\}$ and $^{13}C\{^1H\}$ NMR spectra were recorded on a Bruker ARX-400 spectrometer operating at frequencies of 100, 161 and 400 MHz, respectively. Peak positions are relative to tetramethylsilane and were calibrated against the residual solvent resonance (^1H) or the deuterated solvent multiplet (^{13}C). Phosphorus chemical shifts were measured relative to external 85% H_3PO_4, with downfield shifts reported as positive. ^{11}B NMR spectra were recorded on a Bruker Avance DRX-400 spectrometer operating at 128 MHz. The ^{11}B chemical shifts are relative to an external reference of BF_3 in diethyl ether, with positive values downfield from the reference. All the NMR spectra were recorded at room temperature (20 °C) unless otherwise stated. Elemental analyses (C, H, N) were performed using a Carlo Erba model 1106 elemental analyser by the Microanalytical Service of the Department of Chemistry at the University of Florence.

4.2. Synthesis of [$Cp^*Rh\{N$–B–PTA(BH_3)$\}Cl_2$] (**3**)

4.2.1. Method A

A red suspension of [$Cp^*RhCl(\mu\text{-}Cl)]_2$ (100.0 mg, 0.16 mmol) in THF (30 mL) was treated with solid *N*–*B*–PTA(BH_3) (54.7 mg, 0.32 mmol) at room temperature under stirring. An orange solution was obtained, from which an orange solid quickly precipitated. The solid was separated from the mother liquor by decantation, washed with Et_2O (2 × 3 mL) and dried under vacuum. Yield: 123.2 mg, 80.2%.

4.2.2. Method B

Compound **3** can also be obtained by treating a red suspension of [$Cp^*Rh(PTA)Cl_2$] (100.0 mg, 0.21 mmol) in THF (15 mL) with BH_3.THF (1 M, 0.25 mmol, 250 μL) at room temperature under stirring. The orange solid obtained was separated from the mother liquor by decantation, washed with Et_2O (2 × 3 mL) and dried under vacuum. Yield: 89.3 mg, 88.6%. Anal. Calc. for $C_{16}H_{30}BCl_2N_3PRh$ (480.03 g/mol): C, 40.03; H, 6.30; N, 8.75. Found: C, 40.10; H, 6.24; N, 8.79%. IR (KBr pellets, cm^{-1}): ν_{BH} = 2372 (m), 2317 (w), 2273 (w), ν_{BN} = 1176 (m). ^1H NMR (DMSO-d_6): 0.85–1.50 (br s, BH_3, 3 H, $\omega_{1/2}$ = 345 Hz); 1.64 (d, C_5CH_3, $^4J_{HP}$ = 4.0 Hz, 15H); 3.85–4.50 (m, CH_2, 12H) ppm. $^{31}P\{^1H\}$ NMR (DMSO-d_6): −29.19 (d, $^1J_{PRh}$ = 146.5 Hz) ppm. $^{13}C\{^1H\}$ NMR (DMSO-d_6): 9.1 (s, C_5CH_3); 46.5 (d, CH_2P, $^1J_{CP}$ = 15.5 Hz); 53.1 (d, CH_2P, $^1J_{CP}$ = 18.4 Hz); 69.2 (d, CH_2N, $^3J_{CP}$ = 6.4 Hz); 76.8 (d, CH_2N, $^3J_{CP}$ = 4.2 Hz); 99.2 (dd, C_5CH_3, $^2J_{CP}$ = 7.1 Hz, $^1J_{CRh}$ = 2.8 Hz) ppm. ^{11}B NMR ($CDCl_3$): −9.85 (br, BH_3) ppm.

4.3. Synthesis of [$Cp^*Rh\{N$–B–PTA(BH_3)$\}_2Cl]Cl$ (**4**)

4.3.1. Method A

A mixture of [$Cp^*RhCl(\mu\text{-}Cl)]_2$ (100.0 mg, 0.16 mmol) and *N*–*B*–PTA(BH_3) (123.0 mg, 0.72 mmol) in CH_2Cl_2 (20 mL) was refluxed for 24 h under stirring. The solution was cooled to room temperature and the yellow solid which precipitated out, was separated from the mother liquor by decantation, washed with cold CH_2Cl_2 (2 × 2 mL) and Et_2O (3 × 3 mL), and dried under vacuum. (116.0 mg, 56% yield) [35].

4.3.2. Method B

Compound **4** can also be obtained by treating a solution of [$Cp^*Rh(PTA)_2Cl]Cl$ (120.0 mg, 0.19 mmol) in THF (15 mL) with $BH_3 \cdot THF$ (1 M, 0.60 mmol, 600 μL) at room temperature under stirring. The yellow solid which separated out was washed with Et_2O (2 × 3 mL) and dried under vacuum. Yield: 88.5 mg, 72% [35].

Anal. Calc. for $C_{22}H_{45}B_2Cl_2N_6P_2Rh$ (651.02 g/mol): C, 40.59; H, 6.97; N, 12.91. Found: C, 40.41; H, 6.71; N, 12.69%. IR (KBr pellets, cm^{-1}): ν_{BH} = 2361 (m), 2319 (w), 2270 (w), ν_{BN} = 1161 (m). ^1H NMR (DMSO-d_6): 0.98–1.40 (br s, BH_3, 6H, $\omega_{1/2}$ = 47 Hz); 1.83 (t, C_5CH_3, $^4J_{HP}$ = 3.3 Hz, 15H); 3.85–4.05 (m, CH_2, 6H); 4.27–4.47 (m, CH_2, 12H); 4.57–4.71 ppm (m, CH_2, 6H). $^{31}P\{^1H\}$ NMR (DMSO-d_6): −32.47 (d, $^1J_{PRh}$ = 135.4 Hz) ppm. $^{13}C\{^1H\}$ NMR (DMSO-d_6): 9.9 (s, C_5CH_3); 47.4 (d, CH_2P, $^1J_{CP}$ = 13.5 Hz); 53.4 (d,CH_2P, $^1J_{CP}$ = 16.4 Hz); 68.7 (br s, CH_2N); 76.1 (br s, CH_2N); 105.6 (m, C_5CH_3) ppm.

4.4. Synthesis of [$Cp^*Rh\{$***N-B-***PTA(BH_3)$_2\}Cl_2$] (**7**)

2.5 equiv. of $BH_3 \cdot THF$ (1 M, 0.53 mL, 0.53 mmol) at room temperature, were added to a stirred [$Cp^*Rh(PTA)Cl_2$] (100.0 mg, 0.21 mmol) solution in THF (15 mL). The formation of an orange solid was immediately observed. The reaction was monitored by $^{31}P\{^1H\}$ NMR (DMSO-d_6) and considered completed when a new and unique signal was observed (−30.9 ppm, J_{PRh} = 151.8 Hz). The solid obtained was separated from the mother liquor by decantation and dried under vacuum (86.1 mg, 83.0% yield). Anal. Calc. for $C_{16}H_{33}B_2Cl_2N_3PRh$ (493.86 g/mol): C, 38.91; H, 6.74; N, 8.51%. Found: C, 38.86; H, 6.77; N, 8.48%. IR (KBr pellets, cm^{-1}): ν_{BH} = 2385 (s), 2345 (m), 2278 (m), ν_{BN} = 1164 (m). ^1H NMR (DMSO-d_6): 0.89–1.44 (br s, BH_3, 6H, $\omega_{1/2}$ = 66 Hz); 1.67 (d, C_5CH_3, $^4J_{HP}$ = 4.2 Hz, 15H); 3.70–4.60 (m, CH_2, 12H) ppm. $^{31}P\{^1H\}$ NMR (DMSO-d_6): −30.87 (d, $^1J_{PRh}$ = 151.8 Hz) ppm. ^{11}B NMR ($CDCl_3$): −9.85 (br, BH_3) ppm.

4.5. Synthesis of [$Cp^*Rh\{N$–B–PTA(BH_3)$\}H_2$] (**8**)

4.5.1. Method A

[$Cp^*Rh(PTA)Cl_2$] (0.70 g, 1.50 mmol) was added to degassed absolute EtOH (30 mL). Then an excess of solid $NaBH_4$ (0.37 g, 9.76 mmol) was added portionwise to the solution and the mixture was stirred for 4 h at room temperature in the dark. The solution was concentrated to dryness and the residue was dissolved in benzene (40 mL), and filtrated under argon through a celite plug. The solvent was removed again under vacuum leaving a fine brown solid (489 mg, 79.3% yield).

4.5.2. Method B

Complex **8** may be prepared in comparable yield by replacing [Cp*Rh(PTA)Cl_2] with **1** in the above method. Anal. Calc. for $C_{16}H_{32}BN_3PRh$ (411.14 g/mol): C, 46.74; H, 7.85; N, 10.22. Found: C, 46.71; H, 7.80; N, 10.26%. IR (KBr pellets, cm^{-1}): ν_{BH} = 2371 (m), 2318 (w), 2275 (w); ν_{RhH} = 1964 (m); ν_{BN} = 1170 (m). ^1H NMR (C_6D_6, for the labelling scheme see sketch 1 above): −13.56 (ddm, Rh-*H*, $^2J_{HP}$ = 43.4; $^1J_{HRh}$ = 27.1; $^4J_{HMe}$ = 1.1 Hz, 2H); 2.04 (C_5CH_3, $^4J_{MeP}$ = 2.7; $^3J_{MeRh}$ = 1.6 Hz, 15H); 2.07 (br s, BH_3, 3H); 3.13 (m, Hβ″, $^4J_{Hβ″Hγ′}$ = 1.5; $^4J_{Hβ″Hδ″}$ = 2.0 Hz, 2Hβ″); 3.17 (m, Hβ′, $^2J_{Hβ′Hβ″}$ = 15.6; $^4J_{Hβ′Hγ′}$ = 1.3; $^4J_{Hβ′Hδ′}$ = 1.3; $^2J_{HβP}$ = 1.3 Hz, 2Hβ′); 3.50 (s, Hδ″); 3.53 (m, Hδ, $^2J_{Hδ′Hδ″}$ = 13.7; $^4J_{Hδ′P}$ = 1.5 Hz, Hδ); 3.68 (m, Hα, $^4J_{HαHβ′}$ = 1.2; $^4J_{HαHβ″}$ = 1.2; $^4J_{HαHγ′}$ = 1.1; $^4J_{HαHγ″}$ = 1.1; $^2J_{HαP}$ = 1.1 Hz, 2 Hα); 3.98 (m, Hγ″, $^4J_{Hγ″Hδ″}$ 2.0 Hz, 2Hγ″); 4.15 (m, Hγ, $^2J_{Hγ′Hγ″}$ 13.2; $^4J_{Hγ′Hδ′}$ 1.3; $^4J_{Hγ′P}$ 1.2 Hz, 2Hγ) ppm. $^{31}P\{^1H\}$ NMR (C_6D_6): −18.41 ppm (d, $^1J_{PRh}$ = 155.0); ^{31}P NMR (C_6D_6): −18.41 ppm (dt, $^1J_{PRh}$ = 155.0 Hz, $^2J_{PH}$ = 43.8 Hz). $^{13}C\{^1H\}$ NMR (C_6D_6, for the labelling scheme used see sketch 1): 11.59 (s, C_5CH_3), 54.87 (dd, $^1J_{CP}$ = 21.0; $^2J_{CRh}$ = 2.0, $C_β$); 60.70 (dd, $^1J_{CP}$ = 13.9; $^2J_{CRh}$ = 2.0, $C_α$); 77.36 (d, $^3J_{CP}$ = 6.6, $C_δ$); 77.57 (d, $^3J_{CP}$ = 4.0, Cγ); 97.47 (dd, $^2J_{CP}$ = 3.7; $^1J_{CRh}$ = 2.9, C_5CH_3) ppm. ^{11}B NMR (C_6D_6): −10.78 (br q, $^1J_{BH}$ = 85.0 Hz, BH_3) ppm.

*4.6. Synthesis of [Cp*Rh{N-B–PTA(BH_3)}(η^2-CH_2 = CHPh)] (**10**)*

To a stirred benzene solution (15 mL) of [Cp*Rh{*N–B*–PTA(BH_3)}H_2] (100.0 mg, 0.24 mmol), 32.5 μL (0.29 mmol) of phenylacetylene were added via syringe. The solution was heated to 60 °C for 1.5 h and the volatiles were removed under vacuum leaving a dark oil, which was triturated with Et_2O to yield an orange solid (92 mg, 74.7% yield). Anal. Calc. for $C_{24}H_{38}BN_3PRh$ (513.28 g/mol): C, 56.16; H, 7.46; N, 8.19. Found: C, 56.10; H, 7.44; N, 8.59%. IR (KBr pellets, cm^{-1}): ν_{BH} = 2363 (m), 2309 (w), 2266 (w), $\nu_{C=C}$ = 1594 (w), ν_{BN} = 1166 (m). ^1H NMR (C_6D_6) (intensity ratio 4:1 A/B rotamers). Rotamer A: 1.21-2.47 (br s, BH_3, 3H); 1.42 (br, =CH_2, $1H_{vinyl}$); 1.67 (d, C_5CH_3, $^4J_{HP}$ = 1.7 Hz, 15H); 2.05 (m, =CH_2, $1H_{vinyl}$); 2.64 (dm, PCH_2, $^2J_{HH}$ = 15.1 Hz, 1 H); 2.72 (dm, PCH_2, $^2J_{HH}$ = 15.4 Hz, 1H); 2.89 (dm, PCH_2, $^2J_{HH}$ = 15.1 Hz, 1H); 2.99 (dm, PCH_2, $^2J_{HH}$ = 15.4 Hz, 1H); 3.10 (dm, PCH_2, $^2J_{HH}$ = 15.3 Hz, 1H); 3.39 (br, NCH_2, 2H); 3.40 (dm, PCH_2, $^2J_{HH}$ = 15.3 Hz, 1H); 3.60 (br, =C*H*, $1H_{vinyl}$); 3.75 (dm, NCH_2, $^4J_{HH}$ = 13.2 Hz, 1H); 3.82 (d, NCH_2, $^2J_{HH}$ = 13.2 Hz, 1H); 3.98 (m, NCH_2, 2H); 6.95 (m, C_6H_5, 1H); 7.03 (t, C_6H_5, $^3J_{HH}$ = 7.5 Hz, 2H); 7.26 (d, C_6H_5, $^3J_{HH}$ = 7.5 Hz, 2H) ppm. Signals of rotamer B could not be assigned as they are likely obscured by those of rotamer A. $^{31}P\{^1H\}$ NMR (C_6D_6): Rotamer A: −36.88 (d, $^1J_{PRh}$ = 213.6 Hz) ppm; Rotamer B: −31.62 (d, $^1J_{PRh}$ = 206.0 Hz) ppm. $^{13}C\{^1H\}$ NMR (C_6D_6), Rotamer A: 10.4 (s, C_5CH_3), 26.7 (dd, =CH_2, $^2J_{CP}$ = 14.8 Hz, $^1J_{CRh}$ = 2.8 Hz); 50.2 (d, PCH_2, $^1J_{CP}$ = 13.4 Hz); 50.3 (d, PCH_2, $^1J_{CP}$ = 13.4 Hz); 50.9 (d, =C*H*, $^2J_{CP}$ = 14.1 Hz); 56.8 (d, PCH_2, $^1J_{CP}$ = 9.2 Hz); 70.6 (d, NCH_2, $^3J_{CP}$ = 5.6 Hz); 77.6 (d, NCH_2, $^3J_{CP}$ = 3.5 Hz); 77.7 (d, NCH_2, $^3J_{CP}$ = 3.5 Hz); 96.6 (dd, C_5CH_3, $^2J_{CP}$ = 3.53 Hz, $^1J_{CRh}$ = 2.8 Hz); 125.1 (s, C_{ortho}–C_6H_5); 149.8 (dd, C_{ipso}–C_6H_5, $^3J_{CP}$ = 3.5 Hz, $^2J_{CRh}$ = 2.1 Hz) ppm, (the aromatic C_{para} and C_{meta}signals are probably obscured by the solvent). Rotamer B: Signals of rotamer B are partially superimposed with those of rotamer A.10.3 (s, C_5CH_3), 46.5 (d, =C*H*, $^2J_{CP}$ = 14.1 Hz); 49.6 and 57.3 (m, PCH_2); 78.0, 78.1 (m, NCH_2); 97.0 (C_5CH_3); 123.8 (s, C_{ortho}–C_6H_5); 146.1 (C_{ipso}–C_6H_5) ppm. ^{11}B NMR (C_6D_6): −10.9 (br, BH_3) ppm (both rotamers).

*4.7. Synthesis of [Cp*Rh{N–B–PTA(BH_3)}{η^2-CH_2CHC(O)OEt}] (**11**)*

24.8 μL (0.24 mmol) of ethyl propiolate were added to a stirred benzene solution (15 mL) of [Cp*Rh{*N–B*–PTA(BH_3)}H_2] (100.0 mg, 0.24 mmol). The solution was additionally stirred for 5 min at room temperature, then filtered and evaporated under vacuum to remove the volatiles. The dark oily residue was triturated with EtOH to give an orange solid (73.2 mg, 59.9 % yield). Anal. Calc. for $C_{21}H_{38}BN_3O_2PRh$ (509.24 g/mol): C, 49.53; H, 7.52; N, 8.25. Found: C, 49.60: H, 7.68; N, 8.59%. IR (KBr pellets, cm^{-1}): ν_{BH} = 2356 (m), 2308 (w), 2265 (w), ν_{CO} = 1680 (m), $\nu_{C=C}$ = 1440 (w), ν_{COC} = 1378 (m), ν_{BN} = 1162 (s). ^1H NMR (C_6D_6): (intensity ratio 9:1 A/B rotamers). Rotamer A: 1.08 (t, CH_2CH_3, $^3J_{HH}$ = 7.1 Hz, 3H); 1.59 (d, C_5CH_3, $^4J_{HP}$ = 2.0 Hz, 15H); 1.67 (m, =CH_2, $1H_{vinyl}$); 2.20 (m, =CH_2, $1H_{vinyl}$); 2.36 (m, =C*H*, $1H_{vinyl}$); 3.26 (m, PCH_2, 2H); 3.54 (m, NCH_2, 1/2H); 3.57 (m, NCH_2, 1/2H); 3.77 (m, NCH_2, PCH_2, 1H+2H); 3.86 (m, PCH_2, 2H); 4.05 (t, CH_2CH_3, $^3J_{HH}$ = 7.1 Hz, 2H); 4.14 (m, NCH_2, 3H); 4.23 (m, NCH_2, 1H); 4.27 (m, NCH_2, 2H) ppm. Signals of rotamer B were not observed as they are likely buried under the resonances of rotamer A. $^{31}P\{^1H\}$ NMR (C_6D_6): Rotamer A: −35.17 ppm (d, $^1J_{PRh}$ = 206.1 Hz); Rotamer B: −32.37 ppm (d, $^1J_{PRh}$ = 198.2 Hz). $^{13}C\{^1H\}$ NMR (C_6D_6): 10.20 (s, C_5CH_3); 14.81 (s, CH_2CH_3), 31.06 (dd, =CH_2, $^3J_{CP}$ = 14.8 Hz, $^2J_{CRh}$ = 4.9 Hz); 38.68 (d, =CH, $^3J_{CP}$ = 14.8 Hz); 49.36 (d, PCH_2, $^1J_{CP}$ = 9.9 Hz); 50.39 (s, CH_2CH_3); 70.84 (d, NCH_2, $^3J_{CP}$ = 5.6 Hz); 77.87 (d, NCH_2, $^3J_{CP}$ = 4.2 Hz); 78.13 (d, NCH_2, $^3J_{CP}$ = 3.5 Hz); 96.90 (dd, C_5CH_3, $^2J_{CP}$ = 4.2 Hz, $^1J_{CRh}$ = 2.8 Hz); 178.01 (t, *C*OO, $^4J_{CP}$ = 2.1 Hz) ppm. Signals of rotamer B were not observed as likely masked by those of rotamer A. ^{11}B NMR (C_6D_6): −10.36 ppm (br, BH_3) (both rotamers).

4.8. Crystallography

Crystals were mounted on a Bruker APEX diffractometer, equipped with a CCD detector, for the unit cell and space group determinations. Selected crystallographic and other relevant data are listed in Table 3 and in the deposited cif file.

Data were corrected for Lorentz and polarization factors with the data reduction software SAINT [36] and empirically for absorption using the SADABS program [37].

Table 3
Experimental data for the X-ray diffraction study of compounds **3** and **10**

	3	**10**
Formula	$C_{16}H_{30}BCl_2N_3PRh$	$C_{24}H_{38}BN_3PRh$
Moleculat weight	480.02	513.26
Data collected *T* (K)	295 (2)	295 (2)
Diffractometer	Bruker APEX	
Crystal system	Orthorhombic	Monoclinic
Space group (no.)	*Pcmn* (62)	$P2_1/a$ (14)
a (Å)	7.2370 (6)	16.168 (1)
b (Å)	12.510 (1)	9.1778 (6)
c (Å)	22.120 (2)	17.096 (1)
α (°)	90	90
β (°)	90	107.91(1)
γ (°)	90	90
V (Å^3)	2002.6 (3)	2413.7(3)
Z	4	4
ρ_{calc} (g cm^{-3})	1.592	1.412
μ (mm^{-1})	1.223	0.790
Radiation	Mo Kα (graphite monochrom., λ = 0.71073 Å)	
θ Range (°)	1.84 < θ < 27.44	2.50 < θ < 27.51
Number of data collected	17243	17130
Number of independent data	2091	5517
Number of observed reflections (n_o) [$\|F_o\|^2 > 2.0\sigma(\|F\|^2)$]	1618	4005
Number of parameters refined (n_v)	92	266
R_{int}[a]	0.0986	0.1236
R (observed reflections)[b]	0.0712	0.0831
R_w^2 (observed reflections)[c]	0.1924	0.1664
Goodness-of-fit[d]	1.274	1.114

[a] $R_{int} = \sum|F_o^2 - < F_o^2 >| / \sum F_o^2$.
[b] $R = \sum(|F_o - (1/k)F_c|)/\sum|F_o|$.
[c] $R_w^2 = \{\sum[w(F_o^2 - (1/k)F_c^2)^2] / \sum w|F_o^2|^2]\}^{1/2}$.
[d] GOF=$[\sum_w(F_o^2 - (1/k)F_c^2)^2/(n_o - n_v)]^{1/2}$.

The structures were solved by direct and Fourier methods and refined by full matrix least-squares [38] (the function minimized being $\sum[w(F_o - 1/kF_c)^2]$). For all structures, no extinction correction was deemed necessary. The scattering factors used, corrected for the real and imaginary parts of the anomalous dispersion, were taken from the literature [32]. All calculations were carried out by using the PC version of SHELX-97 [38], WINGX and ORTEP programs [39].

4.9. Structural study of [$Cp^*Rh\{N–B–PTA(BH_3)\}Cl_2$] (**3**)

The data were collected by using ω scans, in steps of 0.5°. For each of the 1363 collected frames, counting time was 20 s.

The cell constants were refined by least-squares, at the end of the data collection, while the space group, determined from the systematic absences, was consistent with both the orthorhombic space group $Pc2_1n$ (no. 33) or its centrosymmetric counterpart $Pcmn$ (no. 62). The structure could be solved in both space groups. However, the refinement in the non-centrosymmetric space group lead to high correlation coefficients between refined parameters and to geometrical parameters with no physical significance (i.e.: chemically equivalent distances, e.g. the P–C separations, were significantly different). Thus the refinement was carried out in the centrosymmetric space group (with only half molecule in the independent unit). The relatively high R factors and esd's are due to the poor quality of the crystals and the molecular disorder. Indeed, the atoms of the Cp^* ligand show rotational disorder as could be inferred by the very large displacements of the carbon atoms in the Cp^* ring plane leading to unphysical, cigar shaped, ADP's.

Thus the final least-squares refinement was carried out using isotropic displacement parameters for the atoms of the Cp^* moiety and anisotropic for the remaining non-hydrogen atoms. The contribution of the hydrogen atoms, in their calculated positions, [C–H = 0.96 (Å), B(H) = 1.5 × B(C_{bonded}) (Å^2)], was included in the refinement using a riding model.

4.10. Structural study of [$Cp^*Rh\{N–B–PTA(BH_3)\}$ (η^2-CH_2 = CHPh)] (**10**)

The space group was determined from the systematic absences, while the cell constants were refined by least-squares, at the end of the data collection. The data were collected by using ω scans, in steps of 0.5°. For each of the 1363 collected frames, counting time was 20 s.

The least-squares refinement was carried out using anisotropic displacement parameters for all non-hydrogen atoms, while the H atoms were included in the refinement using a riding model [C–H = 0.96 (Å), B(H) = aB(C_{bonded}) (Å^2), with a = 1.5 for the CH_3 groups and a = 1.2 for the remaining hydrogen atoms].

Acknowledgements

The authors would like to thank the EC for promoting this scientific activity through the FP5 Research Training Network HYDROCHEM (HPRN-CT-2002-00176). Thanks are also expressed to "FIRENZE HYDROLAB", a project sponsored by Ente Cassa di Risparmio di Firenze, for financial support. S.B. and M.R.-R. thank Xunta de Galicia for a Parga Pondal contract and a postgraduate grant, respectively. Dr. P. Barbaro (ICCOM CNR) is thanked for help in running ^{11}B NMR spectra.

Appendix A. Supplementary material

CCDC-675447 and 675448 contain the supplementary crystallographic data for this paper. These data can be obtained free of charge from The Cambridge Crystallographic Data Centre via www.ccdc.cam.ac.uk/data_request/cif. Supplementary data associated with this article can be found, in the online version, at doi:10.1016/j.jorganchem.2008.04.006.

References

[1] For a review on water-soluble phosphine complexes and their applications in homogeneous catalysis see: N. Pinault, D.W. Bruce, Coord. Chem. Rev. 241 (2003) 1–25.
[2] B. Cornils, W.A. Herrm (Eds.), Aqueous Phase Organometallic Catalysis, 2nd ed., Wiley–VCH, Weinheim, 2004.
[3] (a) D.J. Daigle, A.B. Pepperman Jr., G. Boudreaux, J. Heterocyc. Chem. 11 (1974) 1085–1086;
(b) D.J. Daigle, Inorg. Synth. 32 (1998) 40–45.
[4] For a review on the PTA chemistry covering the literature up to the end of 2003, see: A.D. Phillips, L. Gonsalvi, A. Romerosa, F. Vizza, M. Peruzzini, Coord. Chem. Rev. 248 (2004) 955–993.
[5] (a) For some general references on sustainable chemistry and catalysis, see, for example: I.W.C.E. Arends, R.A. Sheldon, U. Hanefeld, Green Chemistry and Catalysis, Wiley–VCH, Weinheim, D, 2007;
(b) J.P.G. Crespo, C.A.M. Afonso, Green Separation Processes: Fundamentals and Applications, Wiley–VCH, Weinheim, D, 2006;
(c) D.J. Macquarrie, J.H. Clark, Handbook of Green Chemistry and Technology, Blackwell Pub., Oxford, UK, 2002;
(d) M. Lancaster, Green Chemistry: An Introductory Text, RSC, Cambridge, UK, 2002.
[6] (a) A. Romerosa, M. Saoud, T. Campos-Malpartida, C. Lidrissi, M. Serrano-Ruiz, M. Peruzzini, J.A. Garrido, F. García-Maroto, Eur. J. Inorg. Chem. (2007) 2803–2812;
(b) A. Romerosa, T. Campos-Malpartida, C. Lidrissi, M. Saoud, M. Serrano-Ruiz, M. Peruzzini, J.A. Garrido-Cardenas, F. Garcia-Maroto, Inorg. Chem. 45 (2006) 1289–1298;
(c) D.N. Akbayeva, L. Gonsalvi, W. Oberhauser, M. Peruzzini, F. Vizza, P. Brüggeller, A. Romerosa, G. Sava, A. Bergamo, Chem. Commun. (2003) 264–265.
[7] (a) W.H. Ang, E. Daldini, C. Scolaro, R. Scopelliti, L. Juillerat-Jeannerat, P.J. Dyson, Inorg. Chem. 45 (2006) 9006–9013;
(b) C. Scolaro, T.J. Geldbach, S. Rochat, A. Dorcier, C. Gossens, A. Bergamo, M. Cocchietto, I. Tavernelli, G. Sava, U. Rothlisberger, P.J. Dyson, Organometallics 25 (2006) 756–765;
(c) A. Dorcier, P.J. Dyson, C. Gossens, U. Rothlisberger, R. Scopelliti, I. Tavernelli, Organometallics 24 (2005) 2114–2123;
(d) C. Scolaro, A. Bergamo, L. Brescacin, R. Delfino, M. Cocchietto, G. Laurenczy, T.J. Geldbach, G. Sava, P.J. Dyson, J. Med. Chem. 48 (2005) 4161–4171;
(e) C.S. Allardyce, P.J. Dyson, D.J. Ellis, D P.A. Salter, R. Scopelliti, J. Organomet. Chem. 668 (2003) 35–42;
(f) C.S. Allardyce, P.J. Dyson, D.J. Ellis, S.L. Heath, Chem. Commun. (2001) 1396–1397.
[8] A. Dorcier, W. Han Ang, S. Bolaño, L. Gonsalvi, L. Juillerat-Jeannerat, G. Laurenczy, M. Peruzzini, A.D. Phillips, F. Zanobini, P.J. Dyson, Organometallics 25 (2006) 4090–4096.
[9] A. Romerosa, P. Bergamini, V. Bertolasi, A. Canella, M. Cattabriga, R. Gavioli, S. Mañas, N. Mantovani, L. Pellacani, Inorg. Chem. 43 (2004) 905–913.
[10] (a) (R = Me) D.J. Daigle, A.B. Pepperman Jr., J. Heterocycl. Chem. 12 (1975) 579–580;
(b) (R = Et)J.M. Forward, R.J. Staples, C.W. Liu, J.P. Fackler, Acta Crystallogr. C 53 (1997) 195–197;
(c) (R = Bz)E. Fluck, J.E. Förster, J. Weidlein, E. Hädicke, Z. Naturforsch. 32 (1977) 499–506.
[11] (a) D.J. Darensbourg, C.G. Ortiz, J.W. Kamplain, Organometallics 23 (2004) 1747–1754;
(b) D.A. Krogstad, G.S. Ellis, A.K. Gunderson, A.J. Hammrich, J.W. Rudolf, J.A. Halfen, Polyhedron 26 (2007) 4093–4100.
[12] A. Mena-Cruz, P. Lorenzo-Luis, A. Romerosa, M. Saoud, M. Serrano-Ruiz, Inorg. Chem. 46 (2007) 6120–6128.
[13] (a) B. Assmann, K. Angermaier, H. Schmidbaur, J. Chem. Soc., Chem. Commun. (1994) 941–942;
(b) B. Assmann, K. Angermaier, M. Paul, H. Riede, H. Schmidbaur, Chem. Ber. 128 (1995) 891–900.
[14] A.D. Phillips, S. Bolaño, S.S. Bosquain, J.-C. Daran, R. Malacea, M. Peruzzini, R. Poli, L. Gonsalvi, Organometallics 25 (2006) 2189–2200.
[15] S. Bolaño, A. Albinati, J. Bravo, L. Gonsalvi, M. Peruzzini, Inorg. Chem. Commun. 9 (2006) 360–363.
[16] B.J. Frost, C.A. Mebi, P.W. Gingrich, Eur. J. Inorg. Chem. (2006) 1182–1189.
[17] See for example: C.A. Taylor II, S.W. Brown, V. Subramaniam, S. Kidner, S.C. Rand, R. Clarke, Appl. Phys. Lett. 65 (1994) 1251–1253.
[18] Coordination of PTA and its derivatives through nitrogen rather than phosphorus has been also reported see: B.J. Frost, C.M. Bautista, R. Huang, J. Shearer, Inorg. Chem. 45 (2007) 3481–3483;
Nitrogen coordination after metal coordination of the phosphorus donor is also known. See:C. Lidrissi, A. Romerosa, M. Saoud, M. Serrano-Ruiz, L. Gonsalvi, M. Peruzzini, Angew. Chem., Int. Ed. 44 (2005) 2568–2572.

[19] D.J. Darensbourg, N.W. Stafford, F. Joó, J.H. Reibenspies, J. Organomet. Chem. 488 (1995) 99–108.
[20] S. Ogo, T. Suzuki, Y. Ozawa, K. Isobe, Inorg. Chem. 35 (1996) 6093–6101.
[21] The ruthenium derivatives [TpRuX(PPh_3){PTA(BH_3)}] (X = Cl, H) and [TpRuCl{PTA(BH_3)}$_2$][Tp = tris-(pyrazolyl)borate] have been also prepared: S. Bolañ o, J. Bravo, J.A. Castro, M.M. Rodríguez-Rocha, M.F.C. Guedes da Silva, A.J.L. Pombeiro, L. Gonsalvi, M. Peruzzini, Eur. J. Inorg. Chem (2007) 5523–5532.
[22] At room temperature the hydrolysis of **3** to **2** shows an approximate $t_{1/2}$ of ca. 5 h. The formation of H_3BO_3 when **3** is dissolved in water is confirmed by ^{11}B NMR monitoring of the hydrolysis process where a singlet at 19.5 ppm assigned to boric acid appears. See: (a) S. Hermanek, Chem. Rev. 92 (1992) 325–362;
(b) R.R. Gupta, M.D. Lechner, Chemical Shifts and Coupling Constants for Boron-11 and Phosphorus-31 Landolt–Börnstein - Group III Condensed Matter, vol. 35/subvolume A, Springer-Verlag GmbH, 1997.
[23] Spectroscopic data for the *N*–*B*–PTA(BH_3) and *N*–*B*–PTA(BH_3)$_2$ ligands: *N*–B–PTA(BH_3): $^{31}P\{^1H\}$ NMR (161 MHz, acetone-d_6, 20 °C): −95.2 ppm (s); ^1H NMR (400 MHz, acetone-d_6,20 °C): 1.23 (br q, $^1J_{HB}$ = 94 Hz, 3H, BH_3), 3.67–4.04 (m, 6H, PCH_2N), 4.24–4.56 (m, 6H, NCH_2N). *N*–*B*–PTA(BH_3)$_2$: $^{31}P\{^1H\}$ NMR (161 MHz, acetone-d_6, 20 °C): −92.5 ppm (s); ^1H NMR (400 MHz, acetone-d_6, 20 °C): 1.40 (br q, $^1J_{HB}$ = 92 Hz, 6H, BH_3), 3.66–4.63 (m, 12H, CH_2).
[24] (a) A. Bakac, Dalton Trans. (2006) 1589–1596;
(b) X. Fu, B.B. Wayland, J. Am. Chem. Soc. 127 (2005) 16460–16467.
[25] R.A. Periana, R.G. Bergman, J. Am. Chem. Soc. 108 (1986) 7332–7346.
[26] V.I. Bakhmutov, Practical NMR Relaxation for Chemists, Wiley Interscience, Chichester, UK, 2004.
[27] gNMR version 4.1, Cherwell Scientific Limited, Oxford Science Park, Oxford, UK, 1999.
[28] As the reaction of **2** with Red-Al does not afford **9** in quantitative NMR yield, we did not attempt to isolate the dihydride **9** in pure form from this reaction. Minor amounts of other species, summing up to less than 10 % with respect to **9**, whose assignment resulted difficult, were always observed. The most abundant impurities were attributed to a Rh(I) species (δ = −35, d, J_{PRh} = 207 Hz) tentatively assigned as [Cp*Rh(PTA)$_2$] (see [Cp*Rh(CO)(PTA): δ = −37.2, d, J_{PRh} = 187 Hz) [8] and to the deuterido perdeuterated phenyl derivative [Cp*Rh(PTA)D(Ph-d_5)] (^{31}P NMR: δ = −30, d, $J_{PRh}\sim$ 170 Hz) which likely formed from **9** via H_2 reductive elimination followed by C–D oxidative addition from C_6D_6 solvent.
[29] (a) A. Selmeczy, W.D. Jones, Inorg. Chim. Acta 300/302 (2000) 138–150;
(b) C. Bianchini, A. Meli, M. Peruzzini, F. Vizza, P. Frediani, Organometallics 9 (1990) 1146–1155;
(c) B.L. Booth, A.D. Lloyd, J. Organomet. Chem. 35 (1972) 195–201.
[30] (a) G.E. Herberich, H. Mayer, J. Organomet. Chem. 347 (1988) 93–100;
(b) D.L. Reger, S.A. Klaeren, J.E. Babin, R.D. Adams, Organometallics 7 (1988) 181–189;
(c) R.G. Bergman, J.M. Huggins, J. Am. Chem. Soc. 103 (1981) 3002–3011.
[31] B. Klingert, H. Werner, Chem. Ber. 116 (1983) 1450–1462.
[32] A.J.C. Wilson (Ed.), International Tables for X-ray Crystallography, vol. C, Kluwer Academic, Dordrecht, The Netherlands, 1992 (Chapter 9.6).
[33] J.W. Kang, K. Moseley, P.M. Maitlis, J. Am. Chem. Soc. 91 (1969) 5970–5977.
[34] D.D. Perrin, W.L.F. Armarego, Purification of Laboratory Chemicals, 3rd ed., Oxford, Butterworth and Heinemann, 1988.
[35] $P\{^1H\}$ NMR analysis (DMSO-d_6) of the crude product confirms that this solid is an approximate 9:1 mixture of **4** and **3**. The formation of **3** as a contaminant in the attempted isolation of **4** cannot be avoided even when the solution used to precipitate the solid contained only 4 ($^{31}P\{^1H\}$ NMR check).
[36] BrukerAXS, SAINT, Integration Software, Bruker Analytical X-ray Systems, Madison, WI, 1995.
[37] G.M. Sheldrick, SADABS, Program for Absorption Correction, University of Göttingen, Göttingen, Germany, 1996.
[38] G.M. Sheldrick, SHELX-97 Structure Solution and Refinement Package, Universit ät Göttingen, 1997.
[39] (a) L.J. Farrugia, J. Appl. Crystallogr. 30 (1997) 565;
(b) L.J. Farrugia, J. Appl. Crystallogr. 32 (1999) 837.